Time-Frequency Analysis Of Natural Scene Anisotropic Scattering Behavior From Pol-In-SAR Data

L. Ferro-Famil [(1)], A. Reigber [(2)], E. Pottier[(1)]

[(1)] IETR Laboratory, UMR CNRS 6164, Radar Polarimetry Group University of Rennes 1
Campus de Beaulieu – Bâtiment 11D263 Avenue General Leclerc, CS 74205 35042 Rennes Cedex, France
(2) Technical University Berlin, Department of Photogrammetry and Cartography, D-10623 Berlin, Germany,

Abstract

In this paper, a fully polarimetric time-frequency analysis method is introduced to decompose synthesized polarimetric and interferometric SAR images into range-frequency and azimuth-frequency domain. This 4-D representation permits to characterize the frequency response of the scene reflectivity, observed under different azimuth look-angles. A statistical analysis of polarimetric parameters permits to clearly discriminate media showing a non-stationary behavior during the SAR integration. A method is proposed to eliminate the influence of backscattering variations in conventional polarimetric SAR data analysis.

1 Introduction

Complex targets, characterized by anisotropic geometrical structures, may show a varying electromagnetic behavior during SAR integration, since they are illuminated from different positions with different frequency components. In this paper, a scene backscattering response is characterized using range and azimuth frequency atoms, in order to analyze the spectral content of responses of the whole observed scene under specific look-angles. A study of the evolution of polarimetric properties during the SAR integration allows to identify and to eliminate the influence of non-stationary scattering behaviors from full resolution polarimetric signatures.

2 Principle of Range-Azimuth Time-Frequency analysis

2.1 Time-frequency decomposition

The time-frequency approach developed in this study is based on the use of a windowed Fourier transform, or Gabor transform. This kind of transformation permits to decompose an already processed SAR image signal , $S(\mathbf{l})$ into different spectral components, using the analyzing function $g(\mathbf{l})$, as follows :

$$S_{sub}(\mathbf{l_0};\boldsymbol{\omega}_{sub}) = \int S(\mathbf{l}) g(\mathbf{l}-\mathbf{l_0}) e^{j\boldsymbol{\omega}_{sub}(\mathbf{l}-\mathbf{l_0})} \mathbf{dl} \qquad (1)$$

where $\mathbf{l}=[x,y]$ and $\boldsymbol{\omega}=[\omega_x,\omega_y]$ represent positions vectors in time and frequency respectively and the subscript *sub* indicates the component under consideration. The application of a Fourier transform to (1) shows that the spectrum of S_{sub} is given by the product of the SAR image spectrum by the transform of the analyzing function *g* shifted around the frequency vector ω_{sub}. This approach permits to analyze the spectral content of a synthesized SAR response with a resolution limitation given by Heisenberg-Gabor uncertainty relation :

$$\Delta\boldsymbol{\omega}\,\Delta\mathbf{l} = \mathbf{u} \qquad (2)$$

This relation specifies that the time-frequency resolution product equals a constant fixed by the shape of g. The nature of the analyzing function is generally chosen so as to preserve resolution while maintaining sufficiently low side-lobe amplitudes in time domain.

2.2 Azimuth and range decomposition

During SAR image formation, many low resolution echoes of a target, received under different squint angles, are integrated to form the full resolution SAR image. A single pixel in a SAR image corresponds then to a certain range of angles limited by the azimuth antenna pattern. The azimuth look-angle, ϕ, is related to the azimuth frequency by :

$$\omega_x = 2\omega_c \sin\phi \qquad (3)$$

with ω_c denoting the carrier frequency of the radar. Time-frequency decomposition in the azimuth direction consists in processing a set of images containing different parts of the SAR Doppler spectra, with a reduced resolution, but corresponding to different azi-

muth look-angles. A SAR antenna generally emits and receives linearly modulated chirp signals, characterized by a wide frequency spectrum in the case of high resolution data. Received signals correspond then to the response of a scene observed at different frequencies. A spectral analysis in the range direction may reveal frequency sensitive responses due to objects resonant behavior or complex structure.

3 Anisotropic polarimetric behavior

Polarimetric descriptors, such as H and $\underline{\alpha}$ [1], widely used in natural media physical parameter retrieval procedures[2-3], permit to determine in a quantitative way the importance of eventual non-stationary patterns from an applicative point of view. An azimuth decomposition is applied to polarimetric SAR data acquired by the DLR E-SAR sensor, at L band, over the Alling test site, Germany. The original image resolution is 2m in range and 1m in azimuth, corresponding to an azimuthal variation of the look-angle of approximately 7.5 degrees. Fig. 1 shows an example of an azimuth decomposition into independent subspectra over a particular area, corresponding to plowed fields.

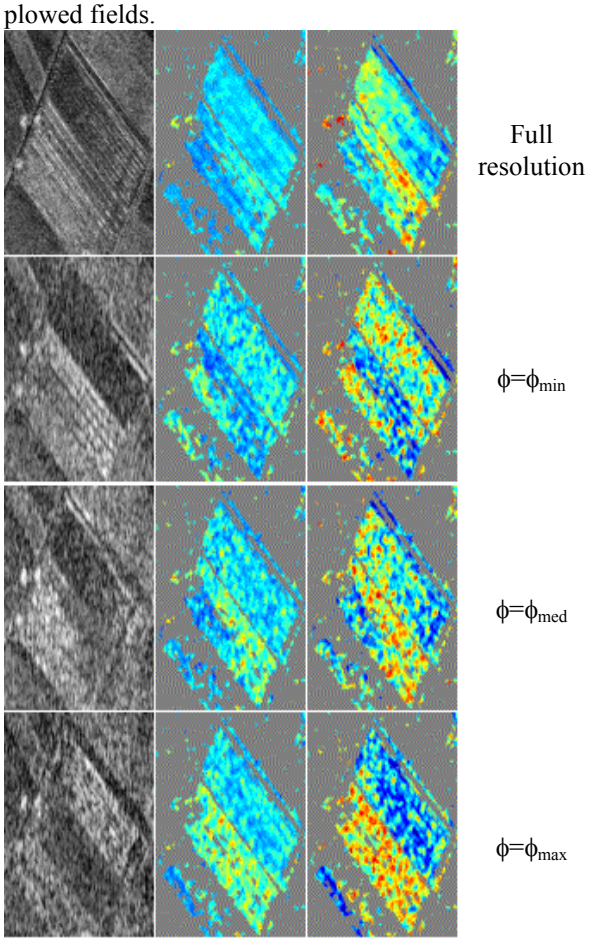

Fig. 1 Polarimetric parameters over isolated fields at full resolution and after azimuth decomposition

Images of the span and H and $\underline{\alpha}$ parameters are represented for different azimuth look-angles and for the full resolution case. Large variations in the scattering mechanism nature and degree of randomness occur as the azimuth look-angle changes. For particular azimuth look-angles, some fields show a sudden change of behavior. The span reaches a maximum value, while the polarimetric indicators H and $\underline{\alpha}$ are characterized by low values. Stripes in the span image indicate that coherent constructive and destructive interferences occur within the pixels and are characteristic of Bragg resonant scattering over periodic surfaces.
A range-azimuth time-frequency analysis is led over 3 points (P_1, P_2, P_3) located at different range positions within a plowed field, Fig.2. Results are represented, for each point into a range frequency and azimuth frequency plane as depicted in Fig.2.

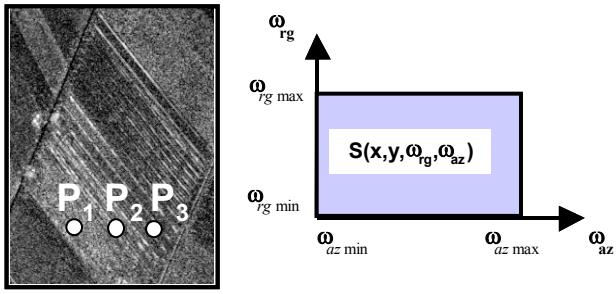

$\theta_1 < \theta_2 < \theta_3$

Fig. 2 : Location of test points (left) range-azimuth frequency representation plane (right)

Time-frequency analysis results represented in Fig. 3 show that the three points under study do not have a stationary range and azimuth scattering behavior. Some $(\omega_{rg}, \omega_{az})$ couples show high span values and low H and $\underline{\alpha}$, characteristic of Bragg resonance.
Bragg resonance phenomenon is due to the coherent summation of simultaneously constructive contributions of a set of scatterers and is likely to happen during the observation of periodic surfaces or irregular surfaces with a strong periodic component. The resonance condition can be written as follows :

$$\cos\phi_0 \; 2k_y = n\frac{2\pi}{P} \quad \Rightarrow \sin\theta\cos\phi_o = n\frac{\lambda}{2P} \qquad (4)$$

where k_y correspond to the component of the incident wavenumber vector parallel to the ground, n is an unknown integer number and P is the surface period. The local incidence angle is denoted θ, while ϕ_o represents the azimuthal angular difference between the observation position and the normal to the rows of the periodic surface.
The time-frequency characteristics of P_2 in Fig. 3 indicate a coupling of the $(\omega_{rg}, \omega_{az})$ coordinates of resonating pixels. This phenomenon is due to the interaction of the $\cos\phi_0$ and λ terms in the Bragg resonance condition enounced in (4). It may also be observed that as the incidence angle increases, from P_1

to P_3, the oblique resonating stripe slides from low azimuth frequencies to higher ones. This displacement of the resonance loci is due to the dependence of the Bragg condition in (4) on the $\sin(\theta)$ term.

It may be noted that polarimetric indicators of pixels that do not belong to resonating stripes are unaffected by the Bragg resonance, are similar to the ones observed over stationary fields.

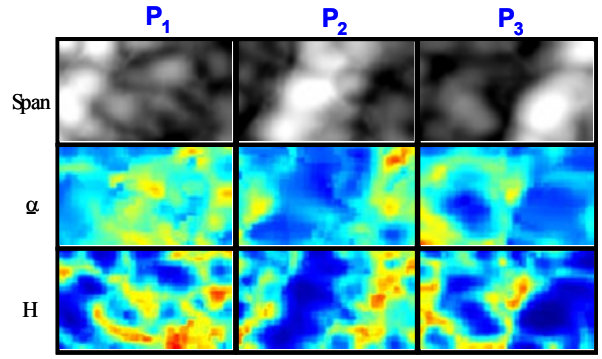

Fig. 3 Representation of polarimetric characteristics in the range-anzimuth spectral domain

4 Anisotropic pol-in behavior

Cloude and Papathanassiou [4] introduced an original formulation of the interferometric coherence using projection vectors to compute the interferometric coherence of a polarization channel in any emitting-receiving polarization basis. Papathanassiou and Cloude [4][5] further developed this concept to define an optimal coherence set $(\gamma_{opt1},\gamma_{opt2},\gamma_{opt3})$, with $\gamma_{opt1} \geq \gamma_{opt2} \geq \gamma_{opt3}$. The optimal coherence set is obtained by analytically tuning the projection vectors, $\mathbf{w_1}$ and $\mathbf{w_2}$, to maximize the modulus of the coherences. The results of the optimization procedure show an enhanced contrast between the different optimal coherences that represent highly descriptive indicators.

An example of non-stationary polarimetric interferometric scattering behavior is described in Fig.4 .

The color-coded images represent the joint information associated to the optimal coherences and reveal particular behaviors of different types of natural medium under examination. White areas indicate targets showing high coherence independently of the polarization. Such a behavior is characteristic of point scatterers and isotropic bare soils. Green zones reveal the presence of a single dominant coherent mechanism within the resolution cell. Secondary coherences, associated to the red and blue channels have significantly lower values. Such zones correspond to surfaces with low SNR or non-stationary responses.

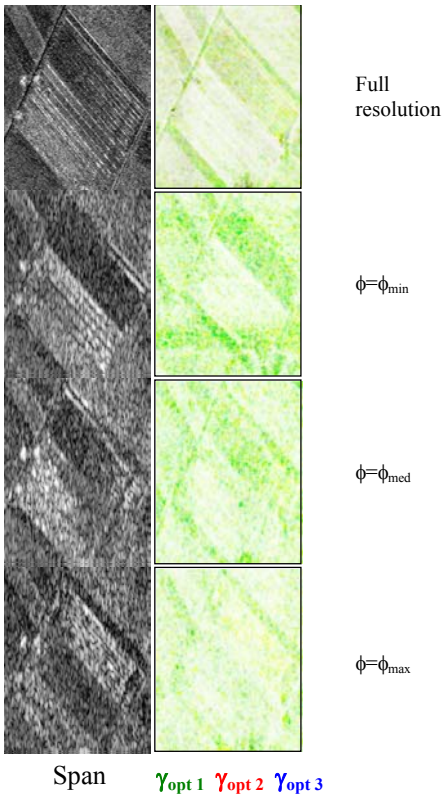

Fig. 4 Polarimetric Interferometric parameters over isolated fields at full resolution and after sub-aperture decomposition

The images of polarimetric interferometic indicators for different sub-spectra displayed in Fig. 4 clearly indicate that coherence is affected by Bragg scattering. Such variations are due to the strong fluctuations of the backscattered intensity. Indeed, as the surface resonates, the Signal to Noise Ratio becomes important and the coherence increases in an important way. Such anisotropic behavior might be a limitation for surface parameter and overlaying vegetation characteristic estimation from polarimetric coherence estimation.

5 Anisotropic media detection and coherent image restoration

A statistical analysis of the scene response over different independent sub-spectra may be used to detect targets showing a non-stationary behavior and locate their position in the spectrum.

Each pixel of the SAR scene is then associated to a set of independent sample coherency matrices. It was shown that a sample n-look coherency matrix, $\mathbf{T}$, follows a complex Wishart probability function with n degrees of freedom, $W_C(n,\mathbf{\Sigma})$. A pixel has a stationary isotropic spectral behavior if its R sub-spectra sample coherency matrices $\mathbf{T_i}$, with $i=1,...,R$, follow the same distribution and fulfill the following hypothesis :

$$. \; Hyp : \mathbf{\Sigma_1} = \ldots = \mathbf{\Sigma_R} \qquad (3)$$

The validity of this hypothesis is tested by means of a maximum likelihood ratio $\mathbf{\Lambda}$, built from the independent coherency matrices as follows :

$$\Lambda = \frac{\prod_{i=1}^{R} |\mathbf{T_i}|^{n_i}}{|\mathbf{T_t}|^{n_t}}, \; n_t = \sum_{i=1}^{R} n_i, \; \mathbf{T_t} = \frac{\sum_{i=1}^{R} n_i \mathbf{T_i}}{n_t} \qquad (4)$$

The variable n_i represents the number of scattering vectors used to compute the sample coherency matrix $\mathbf{T_i}$. The hypothesis is accepted and the target is considered to be isotropic, with an arbitrarily chosen probability of false alarm P_{fa}, if $\Lambda > c_\beta$ with $P_{fa}(c_\beta) = \beta$. The calculation of the ML ratio statistics was derived by Ferro-Famil et al. from the moment function of the ML ratio [6].

A similar approach can be applied to the location of anisotropic characteristics by comparing the contributions of each sub-spectrum image in the global ratio [6]. The application of this algorithm to the Alling data set reveals that a substantial number of pixels have a non-stationary behavior during the SAR integration and successfully determine its position in the Range-Doppler spectrum. Most of the anisotropic scatterers belong to agricultural fields affected by Bragg resonance. Complex targets and diffracting edges, whose scattering characteristics highly depends on the observation position, are discriminated over built-up areas.

Once pixels with anisotropic behavior and the respective problematic sub-apertures are known, one can try to eliminate anisotropic contributions, in order to improve the retrieval of physical properties from polarimetric data. An efficient way consists in equalizing, for each anisotropic pixel, the amplitude of non-stationary sub-apertures to the average amplitude of the unaffected ones [6].

In Fig. 5, polarimetric parameters of the full-resolution SAR image after restoration are shown. The image quality is comparable with the original one, shown in Fig. 1. Differences between polarimetric descriptors, entropy and $\underline{\alpha}$, evaluated in the original and restored images can be observed. Maximal variations of 70° and 0.8 are observed, over anisotropic point scatterers, for $|\Delta\underline{\alpha}|$ and $|\Delta H|$ respectively. Over non-stationary fields affected by Bragg-scattering, the average variations in $|\Delta\underline{\alpha}|$ and $|\Delta H|$ are respectively 7° and 0.2. Such values are significant with respect to the ranges of the polarimetric indicators, which in case surface scattering equal 40° for $\underline{\alpha}$ and 0.9 for the entropy.

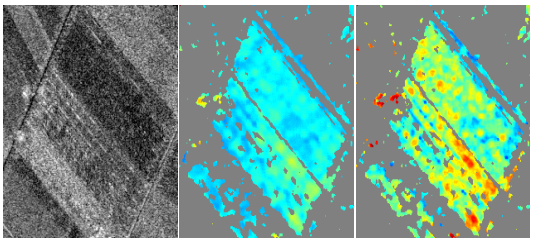

Fig. 5 Polarimetric parameters over isolated fields at full resolution after restoration

5. Conclusion

Time-frequency analysis of fully polarimetric interferometric SAR data is an interesting and important way to characterize the scattering behavior of many targets. As shown in this paper, the effect of pol-in non-stationary may not be neglected in an analysis of anisotropic media without introducing severe errors. Particularly, the characterization of agricultural scenes with polarimetric interferometric descriptors can be heavily influenced by Bragg scattering on periodic surface. In this paper a method is proposed to detect problematic spectral domains, using multi-image ML test statistics. Results of this method are used to minimize the influence of azimuthal backscattering variations in conventional polarimetric SAR data analysis.

6. References

[1] Cloude , S. R. and E. Pottier: “An Entropy Based Classification Scheme for Land Applications of Polarimetric SAR ", *IEEE Tr. on Geosc. and Rem. Sens.*, Vol. 35, No. 1, pp 68-78, January 1997.

[2] Hajnsek, I., "Inversion of Surface Parameters using Polarimetric SAR", Ph.D. Thesis, University Jena, Institute of Geography, Department of Geoinformatik, Jena, Germany, September 2001.

[3] Allain, S., L.Ferro-Famil, E. Pottier, I. Hajnsek," Extraction of Surface Parameters from Multi-frequency and Polarimetric SAR Data", Proc. IGARSS 2002, Toronto, Canada, June 2002.

[4] Cloude, S. R. and K. P. Papathanassiou, "Polarimetric SAR interferometry", IEEE Trans. Geosci. Remote Sensing, vol. 36, no. 5, pp. 1551-1565, September 1998.

[5] Papathanassiou, K. P. and S. R. Cloude, "Single-baseline polarimetric SAR interferometry", IEEE Trans. Geosci. Remote Sensing, vol. 39, no. 11, pp. 2352-2363, November 2001.

[6] Ferro-Famil, L., A. Reigber, E. Pottier, W. M. Boerner, " Scene characterization using subaperture polarimetric SAR data”, *IEEE Tr. on Geosc. and Rem. Sens.*, Vol. 41, No. 10, pp 2264-2276, October 2003.